

er the incorporation of  $^{14}\text{C}$ -labeled amino acid lysine into newly synthesized immunoglobulin. Since the murine lines secrete 10 to 50  $\mu\text{g}$  of immunoglobulin per milliliter (9), it is reasonable to assume that our human myeloma cells secrete similar quantities (10).

An intensive effort has been made to develop human myeloma cell lines for the production of monoclonal antibodies. Although the availability of mouse myeloma cell lines enabled the development of monoclonal antibodies against a wide range of antigens, the use of rodent antibodies for human immunotherapy is limited. It is probably impossible to obtain stable interspecies hybridomas, such as mouse-human, that secrete human antibodies, because the human chromosomes are lost in such hybridomas (11).

One group of investigators reported the development of human monoclonal antibodies (to dinitrochlorobenzene) using the IgE  $\lambda$  myeloma cell line U266 (12); the failure to reproduce these results has been blamed on a latent infection of these myeloma cells by mycoplasma (13). Another group reported the production of human monoclonal antibodies by use of the GM1500 line, which had been derived from a patient with multiple myeloma (14); these results have not been reproduced, probably because the cell line, rather than being a myeloma, is a lymphoblastoid line that is EBNA-positive (15). Like other EBNA-positive B lymphoblast cell lines, they probably produce only small amounts of immunoglobulin. Furthermore because of their latent infection with EBV, such lines may be unstable. Therefore, it appears that so far a human counterpart to the mouse and rat (16) myeloma cell lines does not exist. Cells of our unique line should provide an opportunity for detailed study of the cytogenetics of myeloma, as well as an ideal fusion partner for the production of human monoclonal antibodies.

ABRAHAM KARPAS

Department of Haematological  
Medicine, Cambridge University  
Clinical School, Cambridge CB2 2QL,  
United Kingdom

PATRICIA FISCHER

Department of Haematological  
Medicine, Cambridge University  
Clinical School, Cambridge CB2 2QL,  
United Kingdom, and Cancer Institute,  
University of Vienna, Vienna, Austria

DAVID SWIRSKY

Department of Haematological  
Medicine, Cambridge University  
Clinical School, Cambridge CB2 2QL,  
United Kingdom

#### References and Notes

1. K. Nilsson, H. Bennich, S. G. O. Johansson, J. Ponten, *Clin. Exp. Immunol.* **7**, 477 (1970).
2. A. Karpas, in *The Role of Viruses in Human Cancer*, G. Giraldo and E. Beth (Elsevier/North-Holland, Amsterdam, 1980), pp. 185-203.
3. G. Köhler and C. Milstein, *Nature (London)* **256**, 495 (1975).
4. A. Karpas, F. G. J. Hayhoe, J. Greenberger, C. R. Barker, J. C. Cawley, R. M. Lowenthal, W. C. Moloney, *Leuk. Res.* **1**, 35 (1977).
5. B. M. Reedman and G. Klein, *Int. J. Cancer* **11**, 499 (1973).
6. H. Van Den Berghe, A. Louwaghe, A. Broeck-aert-Van Orshoven, G. David, R. Verwilghen, J. L. Michaux, G. Sokal, *J. Natl. Cancer Inst.* **63**, 11 (1979).
7. K. Nilsson, in *The Epstein-Barr Virus*, M. A. Epstein and B. C. Achong, Eds. (Springer-Verlag, New York, 1980), pp. 225-281.
8. J. Gordon, D. Hough, A. Karpas, J. L. Smith, *Immunology* **32**, 559 (1977).
9. C. Milstein, personal communication.
10. A. Karpas, P. Fischer, D. Swirsky, *Lancet*, in press.
11. C. M. Croce, M. Shander, J. Martinis, L. Cicurel, G. G. D'Ancona, H. Koprowski, *Eur. J. Immunol.* **10**, 486 (1980).
12. L. Olsson and H. S. Kaplan, *Proc. Natl. Acad. Sci. U.S.A.* **77**, 5429 (1980).
13. R. Lewin, *Science* **212**, 767 (1981).
14. C. M. Croce, A. Linnenbach, W. Hall, Z. Steplewski, H. Koprowski, *Nature (London)* **288**, 488 (1980).
15. D. W. Buck, personal communication.
16. G. Galfre, C. Milstein, B. Wright, *Nature (London)* **277**, 131 (1979).
17. We thank F. G. J. Hayhoe for allowing us to study his patient's cells, M. Aveyard and G. Ganster for technical help, O. Haas and P. Breit for help with the preparation of the karyotype, and D. Voak for typology of histocompatibility antigens.

15 January 1982; revised 8 March 1982

## Ribosomal Crystalline Arrays of Large Subunits from *Escherichia coli*

**Abstract.** Crystalline sheets of the 50S ribosomal subunits of *Escherichia coli* have been formed *in vitro*. Electron micrographs of these arrays diffract to 35-angstrom resolution. The lattice parameters of the crystals are  $a = 330 \pm 20$  angstroms,  $b = 330 \pm 30$  angstroms, and  $\alpha = 123^\circ \pm 5^\circ$ , and the space group is most likely  $p21$ . These arrays of ribosomal subunits are sufficiently ordered to resolve such known features of the large ribosomal subunit as the L7/L12 stalk and the central protuberance.

One of the principal requirements for understanding the molecular events that occur during protein synthesis is the determination of the three-dimensional structure of the ribosome. In this report, we describe conditions for the growth *in vitro* of crystalline arrays of large ribosomal subunits from *Escherichia coli*. These microcrystals of ribosomes are sufficiently well ordered to allow the calculation of a density map with 40-Å resolution by three-dimensional reconstruction from electron micrographs. Crystalline arrays formed *in vivo* in eukaryotes have been isolated and analyzed by three-dimensional reconstruction (1, 2) and crystalline arrays of prokaryotic ribosomes have been grown *in vitro* (3-5). However, the microcrystals we grew diffract to a considerably higher resolution than any previously reported. Their symmetry and unit cell dimensions have been characterized. Since they are grown *in vitro* from *E. coli* subunits, they offer the optimal opportunities for correlating biochemical and functional information with structural studies. The arrays are nearly ideal for analysis by three-dimensional reconstruction.

When solutions of 50S ribosomal subunits are maintained in vapor diffusion wells in the presence of ethanol (see legend to Fig. 1 for buffer conditions), a particulate suspension forms at the bottom of the wells within 2 weeks. After 1 to 2 months, the suspension, when ex-

amined by electron microscopy, contains closed tubes (Fig. 1A) and crystalline sheets one or more layers thick (Fig. 1B). Optical and computer-calculated diffraction patterns indicate that the unit cell dimensions, symmetry, and packing are the same in the sheets and the tubes.

Tubes, when negatively stained, flatten on the carbon support films used for electron microscopy to produce "two-sided" images [for example, see (6)]. The flattened tubes are 1750 Å in diameter and of variable length (4000 to 40,000 Å). In the approximately meridionally symmetric optical diffraction pattern shown in Fig. 1C, reflections from one side of the tube have been circled. These reflections index on a primitive lattice with parameters  $a = 330 \pm 20$  Å,  $b = 330 \pm 30$  Å, and  $\alpha = 123^\circ \pm 5^\circ$ . Optical and computer-filtered images of tubes (Fig. 1E) suggest that the symmetry, in projection, is  $p2$ , corresponding to space group  $p21$  (7). The projected structure can also be referred to a centered lattice with approximate symmetry  $cmm$  corresponding to space group  $c222$ . Analysis of the calculated three-dimensional Fourier transform, however, favors a three-dimensional symmetry of  $p21$ , but does not completely exclude  $c222$  (Fig. 2). In addition, by using the lower symmetry space group ( $p21$ ), we do not rule out the additional symmetry elements contained in  $c222$ .

Present in the backgrounds of electron

micrographs are symmetric clusters of subunits (morphological units). Several of these are indicated by arrowheads in the central field in Fig. 1A, and enlargements of them are shown in Fig. 1D. Individual morphological units preferentially orient on the carbon support film with their dyad axis perpendicular to the plane of the film; their profiles closely resemble those seen in the filtered images (Fig. 1E). Crystallization might proceed from these morphological units, since they are commonly found in association with the crystals. Consideration of the size of a ribosomal subunit suggests that if the symmetry is p21, the

asymmetric unit is most likely composed of two 50S subunits. Together, two symmetry-related asymmetric units (containing four subunits in all) form a morphological unit.

The integrity of the 50S ribosomal subunits, as characterized by sedimentation through sucrose gradients and by electron microscopy, was preserved after crystallization [same conditions as in (3)]. When the mother liquor was removed from the well and the remaining microcrystals were redissolved in the gradient buffer (or when the suspension was taken, pelleted from the mother liquor, and redissolved in gradient buffer)

the redissolved microcrystals gave sedimentation profiles indistinguishable from those of control 50S ribosomes and were calculated to contain less than 3 percent (measured by absorbance at 256 nm) 30S or other contaminants. They also were functional in polyphenylalanine synthesis [for conditions, see (8)]. In addition, 50S ribosomes from vapor diffusion wells appear normal when examined by electron microscopy. Hence, the morphology and function of subunits is not significantly altered during the relatively long periods in the vapor diffusion wells.

These microcrystals of *E. coli* 50S ribosomes formed in vitro should be use-

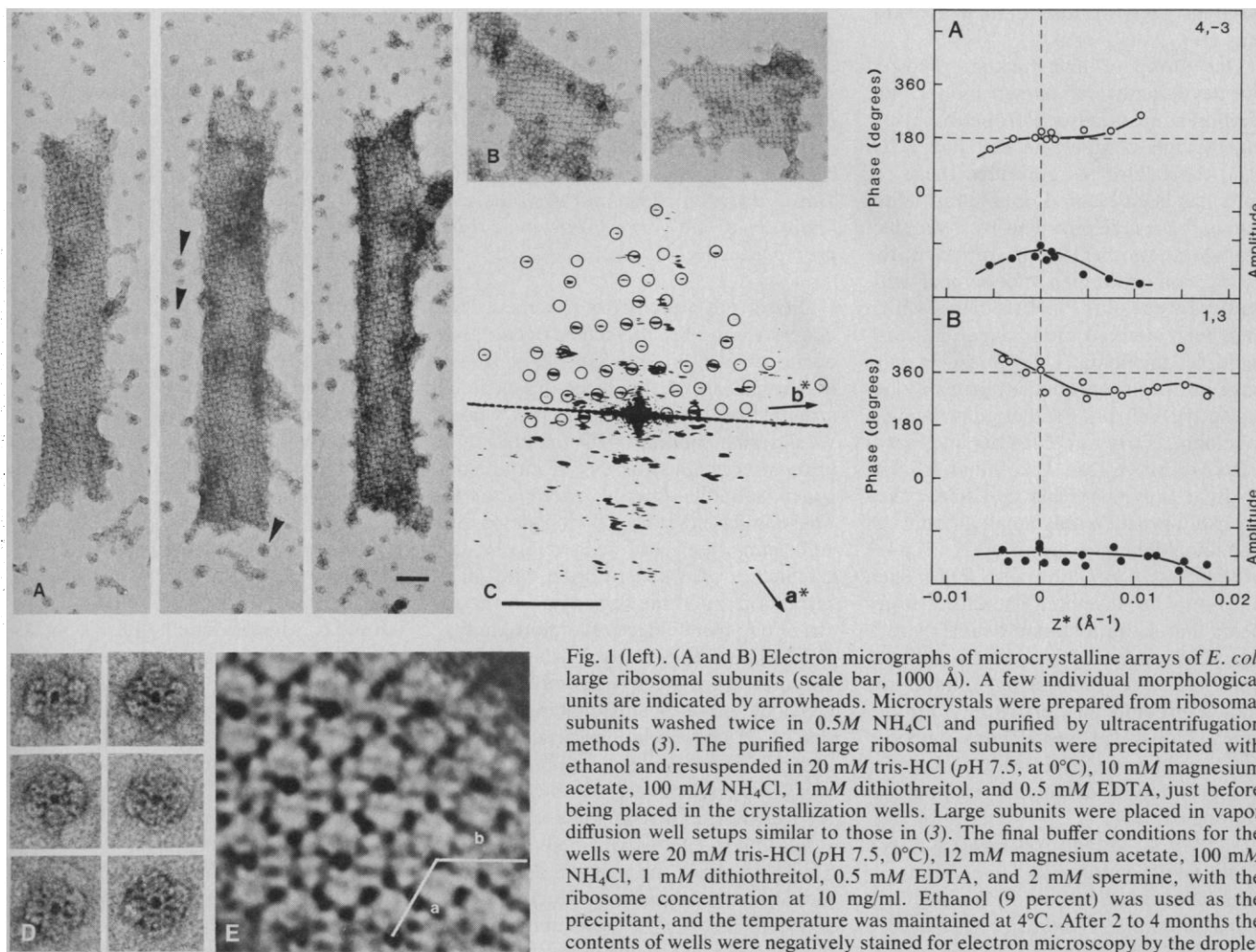


Fig. 1 (left). (A and B) Electron micrographs of microcrystalline arrays of *E. coli* large ribosomal subunits (scale bar, 1000 Å). A few individual morphological units are indicated by arrowheads. Microcrystals were prepared from ribosomal subunits washed twice in 0.5M NH<sub>4</sub>Cl and purified by ultracentrifugation methods (3). The purified large ribosomal subunits were precipitated with ethanol and resuspended in 20 mM tris-HCl (pH 7.5, at 0°C), 10 mM magnesium acetate, 100 mM NH<sub>4</sub>Cl, 1 mM dithiothreitol, and 0.5 mM EDTA, just before being placed in the crystallization wells. Large subunits were placed in vapor diffusion well setups similar to those in (3). The final buffer conditions for the wells were 20 mM tris-HCl (pH 7.5, 0°C), 12 mM magnesium acetate, 100 mM NH<sub>4</sub>Cl, 1 mM dithiothreitol, 0.5 mM EDTA, and 2 mM spermine, with the ribosome concentration at 10 mg/ml. Ethanol (9 percent) was used as the precipitant, and the temperature was maintained at 4°C. After 2 to 4 months the contents of wells were negatively stained for electron microscopy by the droplet method. (C) Optical diffraction pattern of the central electron micrograph shown

in (A). Reflections from one side of the pattern are circled. In addition, the  $a^*$  and  $b^*$  axes ( $a^*$  is perpendicular to  $b$  and  $b^*$  is perpendicular to  $a$ ) have been labeled. Scale bar,  $1/100 \text{ \AA}^{-1}$ . (D) A gallery of electron micrographs of morphological units containing four subunits. The units are oriented as in (B). (E) An optically filtered image of the electron micrograph in (A). The edges  $a$  and  $b$  of a unit cell are marked, with the origin taken as the center of a morphological unit. Fig. 2 (right). The three-dimensional Fourier transform was calculated from a tilt series from several crystals in order to investigate the three-dimensional crystal symmetry. Computer-calculated amplitudes and phases (A) for the (4, -3) reflection and (B) for the (1,3) reflection.  $Z^*$  is the diffracted perpendicular to the plane of the array. The three-dimensional transform was calculated from a tilt series obtained from two different arrays. Each phase (○) and magnitude (●) represents a reflection calculated from a different image. Phases are referenced to a common three-dimensional origin [for example, see (1, 7)] located on a twofold axis, but are otherwise independent measurements. The transform along each  $Z^*$  line has the property  $F_{hk}(Z^*) = F_{hk}^*(-Z^*)$ , confirming the presence of a twofold axis perpendicular to the plane of the array. The transform does not have c222 symmetry, however. If a twofold axis existed in the  $a^*$  direction, then  $F_{1,3}(Z^*)$  should equal  $F_{4,-3}(-Z^*)$  (similar relations should also hold for the other pairs of mirror-related reflections). This was not observed for approximately ten pairs and, in particular, was not found for the pair shown in (A) and (B). Hence we conclude that the true three-dimensional symmetry is probably p21 rather than c222.

ful for study by three-dimensional reconstruction. They have sufficient order for tilting studies and have relatively strong diffraction to resolutions of 35 to 40 Å. They are composed of *E. coli* components and hence the immunological and biochemical approaches developed for them can be applied to the crystals. For example, specific regions of ribosomes may be labeled by Fab antibody tags against proteins and RNA [for a review, see (9)] to determine their positions directly by diffraction techniques. With a three-dimensional map at 50-Å resolution, our preliminary experiments suggest that it is possible to investigate the shapes and mutual orientations of such features as the L7/L12 stalk (10), the central protuberance [the likely site of peptidyl transfer (4)] and the L1 ridge (11). Moreover, the *E. coli* ribosome offers optimal opportunities for correlating results from structural studies with other information. From the degree of order found in these electron micrographs, it also seems possible that single crystals suitable for x-ray diffraction might be obtained.

MICHAEL W. CLARK  
Molecular Biology Institute and  
Department of Biology, University of  
California, Los Angeles 90024

KEVIN LEONARD  
European Molecular Biology  
Laboratory, Heidelberg, Germany

JAMES A. LAKE  
Molecular Biology Institute and  
Department of Biology,  
University of California

#### References and Notes

1. P. N. T. Unwin, *Nature (London)* **269**, 118 (1977).
2. J. A. Lake and H. S. Slayter, *J. Mol. Biol.* **66**, 271 (1972).
3. M. W. Clark, M. Hammons, J. A. Langer, J. A. Lake, *ibid.* **135**, 507 (1979).
4. J. A. Lake, in *Ribosomes: Structure, Function, and Genetics*, G. Chambliss *et al.*, Eds. (University Park Press, Baltimore, 1979), pp. 207-236.
5. A. E. Yonath, J. Mussig, B. Tesche, S. Lorenz, V. A. Erdmann, H. G. Wittmann, *Biochem. Int.* **1**, 428 (1980).
6. D. J. DeRosier and A. Klug, *Nature (London)* **217**, 130 (1968).
7. The nomenclature of the 17 two-sided plane groups is that of S. P. Fuller, R. A. Capoldi, and R. A. Henderson [*J. Mol. Biol.* **134**, 305 (1979)].
8. R. F. Gesteland, *ibid.* **18**, 356 (1966).
9. D. Winkelmann and L. Kahan, in *Ribosomes: Structure, Function, and Genetics*, G. Chambliss *et al.*, Eds. (University Park Press, Baltimore, 1979), pp. 255-265.
10. W. A. Strycharz, M. Nomura, J. A. Lake, *J. Mol. Biol.* **126**, 123 (1978).
11. J. A. Lake and W. A. Strycharz, *ibid.* **153**, 979 (1981).
12. We thank D. Williams and J. Beyer for electron microscopy and photography. Supported by grant PCM 76-14718 from the National Science Foundation and grant GM-24-34 from the National Institute of General Medical Sciences (to J.A.L.), and by PHS national research award 07104 (to M.W.C.). We thank J. Washizaki for photography and D. Eisenberg and D. L. D. Caspar for advice.

5 March 1982

## Spectral Character of Sunlight Modulates Photosynthesis of Previtamin D<sub>3</sub> and Its Photoisomers in Human Skin

**Abstract.** *The photosynthesis of previtamin D<sub>3</sub> from 7-dehydrocholesterol in human skin was determined after exposure to narrow-band radiation or simulated solar radiation. The optimum wavelengths for the production of previtamin D<sub>3</sub> were determined to be between 295 and 300 nanometers. When human skin was exposed to 295-nanometer radiation, up to 65 percent of the original 7-dehydrocholesterol content was converted to previtamin D<sub>3</sub>. In comparison, when adjacent skin was exposed to simulated solar radiation, the maximum formation of previtamin D<sub>3</sub> was about 20 percent. Major differences in the formation of lumisterol<sub>3</sub> and tachysterol<sub>3</sub> from previtamin D<sub>3</sub> were also observed. It is concluded that the spectral character of natural sunlight has a profound effect on the photochemistry of 7-dehydrocholesterol in human skin.*

Man, evolving in an environment bathed in sunlight, developed a variety of physiological responses to solar radiation. One of the best characterized sunlight-mediated cutaneous events in man is the photosynthesis of vitamin D<sub>3</sub>. Exposure to sunlight causes the photochemical transformation of 7-dehydrocholesterol (7-DHC) to previtamin D<sub>3</sub> (preD<sub>3</sub>) in human skin (1). The preD<sub>3</sub> isomerizes by heat to vitamin D<sub>3</sub> or by ultraviolet (UV) radiation to lumisterol<sub>3</sub> and tachysterol<sub>3</sub> (Fig. 1A). The isomerizations of preD<sub>3</sub>, lumisterol<sub>3</sub>, and tachysterol<sub>3</sub> are photoreversible reactions and therefore determine in part the yield of preD<sub>3</sub> and, ultimately, of vitamin D<sub>3</sub> that is produced in the skin. Equipped with the capability of carefully monitoring this well-defined photochemical event in human skin, we investigated the effect of monochromatic radiation on this photochemical reaction and compared it with that resulting from exposure to simulated sunlight. We observed that there were major differences in both the conversion of 7-DHC to preD<sub>3</sub> and the photoisomerization of preD<sub>3</sub> to lumisterol<sub>3</sub> and tachysterol<sub>3</sub> in human epidermis exposed to narrow-band (295-nm) radiation compared with epidermis exposed to simulated or natural solar radiation. We report that the spectral character of natural sunlight is an important factor that modulates the photosynthesis of preD<sub>3</sub>, lumisterol<sub>3</sub>, and tachysterol<sub>3</sub> in human skin.

Surgically obtained type III human skin was separated by heat (1, 2) and then exposed at room temperature to narrow-band radiation, obtained from a 5-kW xenon arc lamp and a monochromator system (Jobin-Yvon HL300), with a half-band width of either 5 or 3 nm. Immediately after irradiation, epidermal lipids were extracted and chromatographed to determine the amount of 7-DHC and its photoproducts (1-3). Figure 1B illustrates an action spectrum thus

obtained for the production of preD<sub>3</sub> from 7-DHC in human epidermis. The optimum wavelengths for the production of preD<sub>3</sub> are between 295 and 300 nm, with an apparent maximum near 297 nm, results similar to those obtained in the rat and in organic solvents (4-7).

Having established that narrow-band, 295- to 300-nm radiation optimally produces preD<sub>3</sub> in human skin, we exposed adjacent, paired samples of human skin to increasing doses of either monochromatic radiation (295 ± 5 nm) or simulated solar UV radiation comparable to that striking the earth at 0° latitude in June at noon (2). With exposure to 295-nm radiation, the maximum possible conversion of 7-DHC to preD<sub>3</sub> in human epidermis was approximately 60 ± 5 percent of the original concentration of 7-DHC (Fig. 2A). At this time, a quasi-photostationary state was established with tachysterol<sub>3</sub>, lumisterol<sub>3</sub>, and 7-DHC representing 25 to 30, 5 to 10, and 2 to 5 percent, respectively (Fig. 2B). In comparison, when the adjacent skin samples were exposed to an equivalent of 15 to 30 minutes of simulated equatorial solar radiation, the maximum preD<sub>3</sub> produced was only 15 to 20 percent of the original 7-DHC levels (Fig. 2A), and a quasi-photostationary state was established with tachysterol<sub>3</sub>, lumisterol<sub>3</sub>, and 7-DHC representing 3 to 6, 50 to 60, and 10 to 20 percent, respectively (Fig. 2). Thus, in comparison with narrow-band 295-nm radiation, exposure to simulated equatorial solar UV radiation significantly diminished the maximum formation of preD<sub>3</sub> in the epidermis and enhanced its conversion to lumisterol<sub>3</sub>. To determine whether human epidermis itself was responsible for the major differences in photoisomer yield between these sources, crystalline 7-DHC was dissolved in tetrahydrofuran at various concentrations (1 nM to 1 mM) and exposed to radiation of 295 ± 5 nm or to simulated solar radiation. The difference in the